

# High-efficiency intra-cavity sum-frequency-generation in a self-seeded image-rotating nanosecond optical parametric oscillator

Darrell J. Armstrong and Arlee V. Smith

Dept. 1128, Sandia National Laboratories, Albuquerque, NM 87185-1423, USA

## ABSTRACT

We have built and tested a highly efficient source of pulsed 320 nm light based on intra-cavity sum-frequency-generation in a self-injection-seeded image-rotating nanosecond optical parametric oscillator. The four-mirror nonplanar ring optical cavity uses the RISTRA geometry, denoting rotated-image singly-resonant twisted rectangle. The cavity contains a type-II  $xz$ -cut KTP crystal pumped by the 532 nm second harmonic of Nd:YAG to generate an 803 nm signal and 1576 nm idler, and a type-II BBO crystal to sum-frequency mix the 532 nm pump and cavity-resonant 803 nm signal to generate 320 nm light. The cavity is configured so pump light passes first through the BBO crystal and then through the KTP crystal with the 320 nm light exiting through the output coupler following the BBO sum-frequency crystal. The cavity output coupler is designed to be a high reflector at 532 nm, have high transmission at 320 nm, and reflect approximately 85% at 803 nm. With this configuration we've obtained 1064 nm to 320 nm optical-to-optical conversion efficiency of 24% and generated single-frequency  $\lambda = 320$  nm pulses with energies up to 140 mJ.

**Keywords:** Nonlinear optics, optical parametric oscillator, intra-cavity, sum-frequency generation, image rotation, nonplanar ring oscillator

## 1. INTRODUCTION

Efficient, high-energy, tunable, nanosecond UV light sources with good beam quality are required for a wide range of applications, including ground-, airborne-, and satellite-based active remote sensing systems. When the required UV wavelengths cannot be obtained by doubling or tripling the frequency of pulsed lasers, nanosecond optical parametric oscillators (OPO's) are often employed as frequency converters, with their output sum-frequency mixed with the second- or third-harmonic of a near-IR pulsed laser such as Nd:YAG. Unfortunately, sources based on conventional OPO's using this approach are often complex and inefficient. However, by incorporating novel techniques, we've developed an OPO-based source that is efficient and will eventually reduce complexity. We use an OPO based on the RISTRA cavity<sup>1</sup> that contains a crystal for oscillation as well as a crystal for sum-frequency generation (SFG). This type of OPO can generate signal waves with high beam quality, which is essential for high efficiency SFG. We also pulse seed the OPO to achieve single-frequency oscillation, early turn-on with low pump fluence, and the highest possible beam quality.

While high-efficiency UV-SFG for pulse energies  $> 100$  mJ remains challenging, recent advancements in nanosecond OPO technology are increasing its feasibility.<sup>1-3</sup> By employing high Fresnel Number image-rotating cavities, nanosecond OPO's can produce high pulse energies using pump fluences  $\lesssim 2$  J/cm<sup>2</sup>, and contrary to expectations, deliver very good beam quality. In earlier work we mixed the 803 nm signal from a RISTRA OPO with 532 nm light in a crystal external to the cavity to produce single-frequency pulses at  $\lambda = 320$  nm with energies of 190 mJ. This approach achieved 1064 nm to 320 nm conversion efficiency of 21%, where the 1064 nm to 532 nm second harmonic generation (SHG) efficiency was  $\sim 70\%$ .<sup>4</sup>

In this report we present an alternative approach, where the SFG crystal is placed inside the OPO cavity to take advantage of the high intra-cavity signal fluence to realize higher conversion efficiency.\* Various intra-cavity

---

Further author information: Send correspondence to D. J. Armstrong  
E-mail: darmstr@sandia.gov, Telephone: 505 844 4757

\*We provide a partial list of references for previous work on intra-cavity upconversion processes in OPO's. There are many more examples in the literature, some found within the references given here.

upconversion configurations have been investigated experimentally using various pump lasers, including ruby-pumped SHG,<sup>5</sup> mode-locked Nd:YAG pumped SFG,<sup>6,7</sup> mode-locked Ti:Sapphire pumped SFG,<sup>8</sup> and theoretically using plane-wave approximations for separate OPO and SFG crystals,<sup>9</sup> and for one crystal that phasematches for oscillation and SFG.<sup>10</sup> This paper describes an intra-cavity SFG system that obtained 532 nm to 320 nm efficiency of 33%, or starting with SHG efficiency of 70%, 1064 nm to 320 nm efficiency of 24%.

## 2. IMAGE-ROTATING NONPLANAR-RING INTRA-CAVITY SFG OPO

Our intra-cavity SFG OPO is based on a quasi-monolithic 90°-image-rotating four-mirror nonplanar-ring oscillator known as the RISTRA, denoting Rotated Image Singly-Resonant Twisted RectAngle. Detailed descriptions of the RISTRA OPO, including design methodology and its use in extra- and intra-cavity UV generation systems are available elsewhere,<sup>1,4,12,13</sup> so our discussion will be brief. Because high-efficiency UV-SFG requires good beam quality, we'll begin by reviewing image rotation in nanosecond OPO's. We'll then describe the use of self injection seeding for high conversion efficiency.

### 2.1. Improving OPO Beam Quality by Intra-Cavity Image Rotation

Image-rotating OPO cavities can produce high-quality output beams that are largely independent of the effects of poor pump-beam quality, and also largely immune to the effects of the high cavity Fresnel Numbers that necessarily result from using short cavities and large diameter pump beams. However, image rotation alone only provides spatial averaging over irregularities in the pump beam. To produce significant “beam cleanup,” image rotation must work in combination with angle-critical birefringent phasematching. The importance of birefringence is that walkoff between signal and idler waves increases correlation in phase and amplitude of the optical fields across one transverse dimension of the beam.

Beam-cleanup from birefringence in planar OPO cavities can be verified by focussing the OPO's resonated wave, and observing that beam quality in the far field is better in the direction of walkoff, also known as the critical direction. This effect is usually evident for OPO's having cavity Fresnel Numbers  $\mathcal{F} = D^2/\lambda L \gtrsim 30$ , where  $D$  is the diameter of the resonated wave,  $\lambda$  the resonated wavelength, and  $L$  the round-trip length of the cavity. If pump-beam diameter increases so that  $\mathcal{F} \gtrsim 300$ , a typical value for a short OPO cavity pumped by a 6–8 mm beam, the clean-up effect can be dramatic. Although the fluence may appear fragmented due to speckle, the ratio of non-critical to critical far-field angles might exceed ten. Image rotation eliminates this asymmetry by extending the cleanup effects of birefringence to both transverse dimensions of the beam. We've found a rotation angle of 90° is convenient and can be obtained by placing a Dove Prism in a three-mirror ring cavity,<sup>3</sup> but prefer the nonplanar geometry of the RISTRA cavity shown in Figs. 1(a)–(c) because it is simpler and more efficient.

Image rotation is most effective when the pump and resonated wave, typically the signal, are orthogonally polarized and walkoff from each other within the crystal, while the pump and non-resonant wave, typically the idler, co-propagate within the crystal and share the same polarization. For example, in our intra-cavity SFG OPO, we use  $xz$ -cut KTP at  $\theta = 58.4^\circ$  to phasematch  $803(e) + 1576.4(o) \rightarrow 532(o)$ , with the 803 nm signal being the resonated wave. These parameters largely prevent amplitude and phase aberrations of a poor-quality pump beam from being imposed on the resonated signal while allowing the pump “noise” to be carried away by the idler. For effective beam cleanup, the resonated wave must propagate around the cavity enough times for walkoff-displacement and image-rotation to overlap the area of the pump beam, setting a lower limit on pump pulse duration.

### 2.2. Self Injection Seeding for High Pump Depletion and High Efficiency

To obtain the highest possible conversion efficiency in a nanosecond OPO, oscillation must begin the moment the pump pulse arrives. However in a typical free-running OPO, the buildup time for oscillation is a substantial fraction of the duration of the pump pulse, so that much of the pump energy remains unused. Increasing the pump fluence decreases buildup time, but efficiency suffers as the signal and idler mix and convert into pump energy through parametric backconversion. The only way to overcome these losses is to injection-seed the OPO with enough optical power to minimize buildup time, and to minimize backconversion with a well-designed OPO cavity. Rejecting the un-resonated idler-wave from the cavity helps reduce backconversion, an easy task in multi-mirror ring designs like the RISTRA. More difficult is injection seeding with sufficient power, which requires

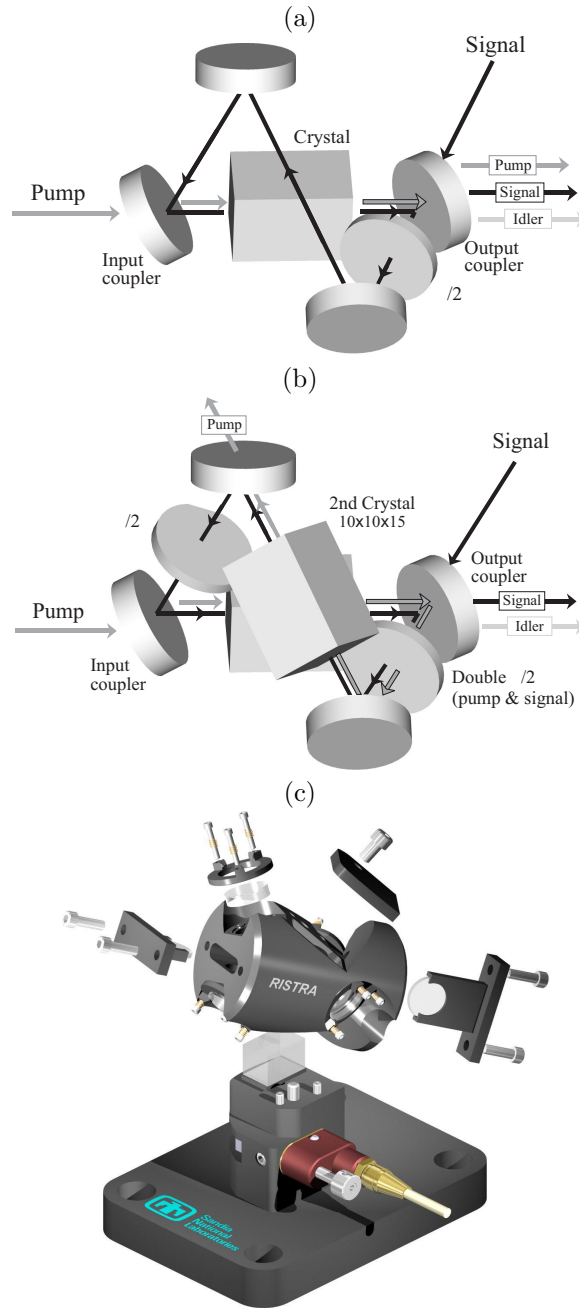


**Figure 1.** Image-rotating four-mirror nonplanar ring-cavity RISTRA OPO. The nonplanar geometry produces  $90^\circ$  of image rotation for each trip around the cavity. It also rotates the polarization so that  $\lambda/2$  plates are required to select cavity polarization equal to the eigenpolarizations of the crystal(s). The lengths of the cavity legs, mirror substrates,  $\lambda/2$  diameters, and crystal dimensions are all to scale. (a) Single-crystal RISTRA. (b) Two-crystal RISTRA. The second crystal requires a second  $\lambda/2$  plate. For the intra-cavity SFG RISTRA the crystal in the lower leg mixes the pump and OPO signal to generate UV, and the second crystal provides oscillation. (c) Quasi-monolithic single-crystal RISTRA cavity. A convenient characteristic of image rotation is insensitivity to tilt of the cavity mirrors. The ring assemblies that secure the cavity mirrors to the cylindrical body provide no adjustment of mirror tilt. The length of the cylindrical body 1.975 in, and the physical cavity length is 109 mm. For a 7 mm diameter pump beam with a flat-top profile and  $\lambda_{\text{signal}} = 803$  nm, the cavity Fresnel Number exceeds 450. See Ref. 3 for additional details.

pulsed seeding. However, the rewards of pulsed seeding outweigh its costs through increased efficiency and lower pump fluence for equivalent output energy, when compared to conventional OPO operation. The reduction in optical damage problems alone can be significant.

To achieve single-frequency pulsed seeding, we begin by injection-seeding the RISTRA cavity at  $\lambda = 803$  nm with a frequency-stabilized cw laser in the “backward direction,” i.e., opposite to the normal direction of oscillation. We then pump backwards with a small-diameter low-energy 532 nm beam from an Nd:YAG laser to generate a low-energy single-frequency pulse. This signal pulse is then resonantly coupled into the cavity in the forward direction before a high-energy forward pump pulse arrives from a second Nd:YAG laser. This form of pulsed seeding, where the OPO generates its own seed pulse, is known as “self seeding.” Another variation of self seeding achieved single longitudinal mode oscillation in a nanosecond OPO by using a high repetition rate pump laser, an optical delay line, and a diffraction grating to spectrally narrow the self-seed pulse.<sup>14</sup> It has also been applied to parametric generation using a long fiber delay-line and tunable fiber Fabry-Perot-Filter.<sup>15</sup>

When a nanosecond OPO is seeded by a pulse, the spatial profile of the seed-pulse can strongly influence the spatial profile of the OPO’s signal beam. This effect is important when the OPO’s signal is used for subsequent mixing such as SFG, where well-matched diameters and spatial profiles result in the highest SFG efficiency. Because we sum-frequency mix using a pump beam with a flat-top spatial profile, our self seed beam must have a flat-top profile as well for maximum efficiency.

To match the diameter and profile of the seed beam to the forward pump, we spatially filter, then collimate and clip the Airy rings to extract the Gaussian-like central disk with diameter  $\approx 4.7$  mm  $1/e^2$ . This beam is injected into a Newport refractive beam shaper, model GBS-AR16, which produces a flat-top Fermi-Dirac profile with diameter  $\approx 8$  mm. This beam is then imaged with slight demagnification into the OPO through the output coupler. The entire process begins with  $\sim 5$  mJ of 803 nm signal leaving the cavity, and ends with the re-injected spatially-conditioned self-seed pulse containing  $\lesssim 400$   $\mu$ J. While spatial conditioning adds complexity, we’ve shown that well-matched flat-top pump and self-seed profiles can result in pump depletion of 85%. We’ve also shown that Gaussian pump and seed profiles, as well as mismatched pump and seed profiles, can substantially diminish pump depletion, resulting in reduced efficiency.<sup>4,12</sup> We have not tested our intra-cavity SFG OPO using spatially mismatched pump and self-seed beams, but we expect the result would be reductions in efficiency comparable to those observed previously.

### 3. EXPERIMENTAL APPARATUS

A simplified block diagram of the experimental apparatus is shown in Fig. 2. The apparatus consists of an intra-cavity SFG RISTRA OPO, a frequency-stabilized cw Ti:Sapphire laser, two Nd:YAG pump lasers, and in the upper right corner of Fig. 2, an optical path for self seeding that was described in Sec. 2.2. The operation of the system begins with the Ti:Sapphire laser injection-seeding the OPO at  $\lambda = 803$  nm to select single longitudinal mode oscillation in the backward direction. The backward-direction Nd:YAG laser then pumps the OPO to generate a low-energy single-frequency pulse. This pulse exits through the output coupler and is subsequently returned to the cavity through the self-seed optical path to pulse-seed the OPO. The forward-propagating high-energy Nd:YAG laser then initiates forward oscillation by amplifying the pulsed seed, and it provides additional energy for generating intra-cavity UV.

Both pump lasers are injection seeded for single-frequency oscillation and have Gaussian-shaped temporal profiles of approximately 10 ns FWHM. We spatially-filter the beam from the oscillator of the backward pump laser (Continuum NY82-10), then frequency-double this output to generate 25–30 mJ in an approximate lowest-order Gaussian profile with  $1/e^2$  diameter of  $\sim 2$  mm. The forward pump laser (Continuum Powerlite 9010) was modified to generate a high-quality flat-top beam with maximum 1064 nm energy of  $\sim 900$  mJ,<sup>16</sup> which is frequency-doubled with  $\sim 70\%$  efficiency in a 7–8 mm diameter beam. The pump lasers are externally triggered to control relative arrival time of their pulses. While a single pump laser can be used for backward- and forward-pumping, external electronic control of each laser greatly simplifies adjusting pulse timing whenever the experimental apparatus is modified. More complete details of the experimental setup can be found in Refs. 4 and 12.

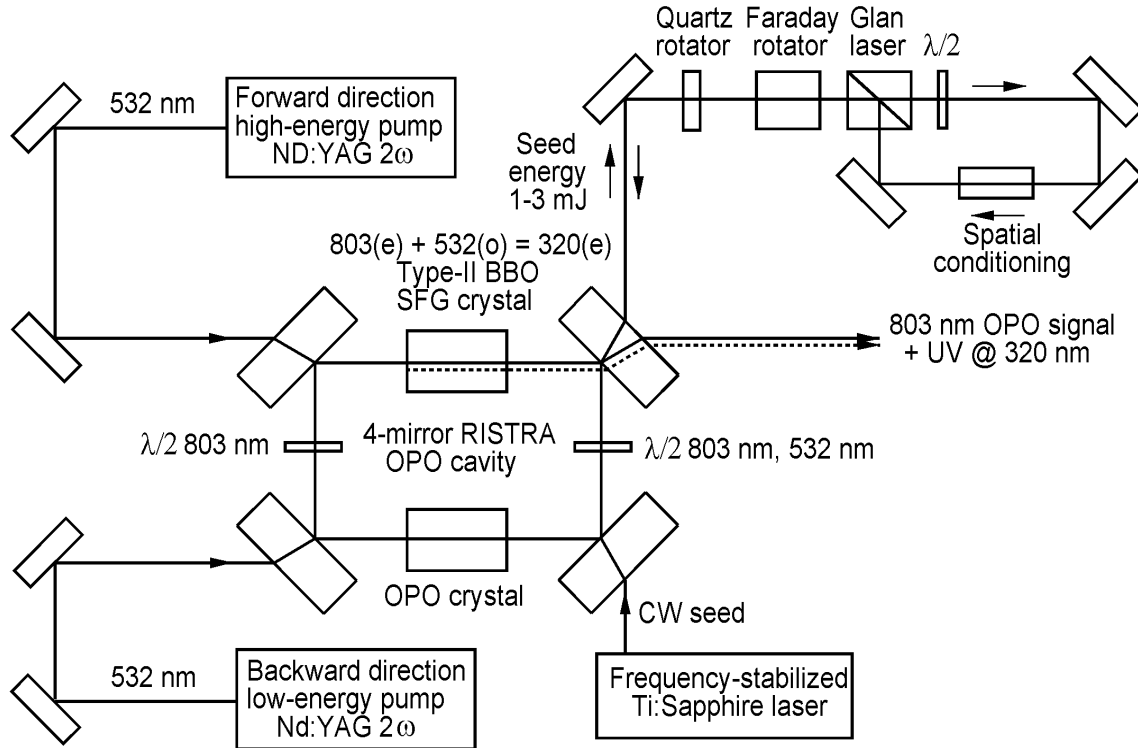


**Figure 2.** (a) Simplified block diagram of self-injection seeded intra-cavity UV generation system based on the RISTRA OPO. The nonplanar RISTRA cavity is projected onto the plane of the page for clarity. The rectangle labelled “Spatial conditioning” consists of a spatial filter, Newport refractive beam shaper, and imaging telescope described in Sec. 2.2.

### 3.1. OPO Specifications

The image-rotating quasi-monolithic RISTRA OPO generates high quality beams and possesses long-term stability, while its four-mirror design ensures singly-resonant oscillation and provides versatility for coupling the seed-, forward-, and backward-pump beams into and out of the cavity. For these reasons it is an ideal choice for self-seeded intra-cavity SFG.

When used as a single- or double-crystal OPO, nominal phasematching parameters involve resonating an *e*-wave for the signal, with the pump and idler *o*-polarized. Alternatively, the resonated wave can be *o*-polarized, with the other two waves *e*-polarized. As described in Sec. 2.1 these combinations of orthogonal polarizations are ideal, but they are not always available, or sometimes are accompanied by smaller than practical  $d_{\text{eff}}$ . Other combinations of *e*- and *o*-waves can be used, but the output beam-quality will then depend more on the beam-quality of the pump. Fortunately for intra-cavity SFG at  $\lambda = 320$  nm, ideal phasematching for oscillation is available in *xz*-cut KTP at  $\theta = 58.4^\circ$  with  $803(e) + 1576.4(o) \rightarrow 532(o)$ . This is combined with SFG in type-II BBO cut at  $\theta = 48.2^\circ$  with  $803(e) + 532(o) \rightarrow 320(e)$ . To obtain the highest SFG efficiency, the SFG crystal is placed in the lower leg of the cavity, so the forward pump passes through it first before being depleted in the OPO crystal. That the SFG-OPO ordering is more efficient than the reverse order was demonstrated earlier,<sup>6</sup> and was confirmed by our numerical models.<sup>11</sup>

In the RISTRA cavities we design for parametric oscillation alone, the nominal output coupler reflectance is 70%. For intra-cavity SFG, higher reflection increases the intra-cavity signal fluence and subsequent SFG efficiency, but durability of dielectric coatings limits the output coupler reflectance to  $\sim 85\%$ . Higher reflectance increases the risk of accidental damage from high signal fluence when the SFG crystal is detuned from  $\Delta k = 0$ . For our OPO the output coupler has  $R_{803\text{nm}} \approx 85\%$ ,  $R_{532\text{nm}} \gtrsim 98\%$ , and  $R_{320\text{nm}} \lesssim 2\%$ .

After selecting our output coupler reflectance, the pump-depleting effects of oscillation and SFG must be balanced by selecting appropriate lengths for the nonlinear crystals. A trial and error approach is impractical due to its prohibitive cost, so the crystal lengths are selected by numerical modelling. While our models are two-dimensional and include walkoff, diffraction, and the image-rotating geometry of the RISTRA cavity, it is impractical to include all of the details encountered in a real experiment, such as stray reflections. Modelling suggested crystal lengths of 15 mm for the  $xz$ -cut KTP, where  $d_{\text{eff}} \approx 3.2$  pm/V, and 10 mm for type-II BBO, where  $d_{\text{eff}} \approx 0.92$  pm/V.

#### 4. RESULTS AND DISCUSSION

By using a RISTRA cavity, the polarizations and crystal angles describe above for optimum beam quality, self seeding for high efficiency, and a pump-beam diameter of 7–8 mm for low fluence, our intra-cavity SFG OPO generated 320 nm pulse energies of 140 mJ with no optical damage, and reliably obtains 532 nm to 320 nm conversion efficiency of 33%. While 140 mJ of UV in a 10 ns pulse might pose a risk of damage with other OPO designs, the fluence in our  $\sim 7$  mm diameter flat-top profile is always  $< 0.5$  J/cm<sup>2</sup>, well below typical damage thresholds for crystals and dielectric coatings.

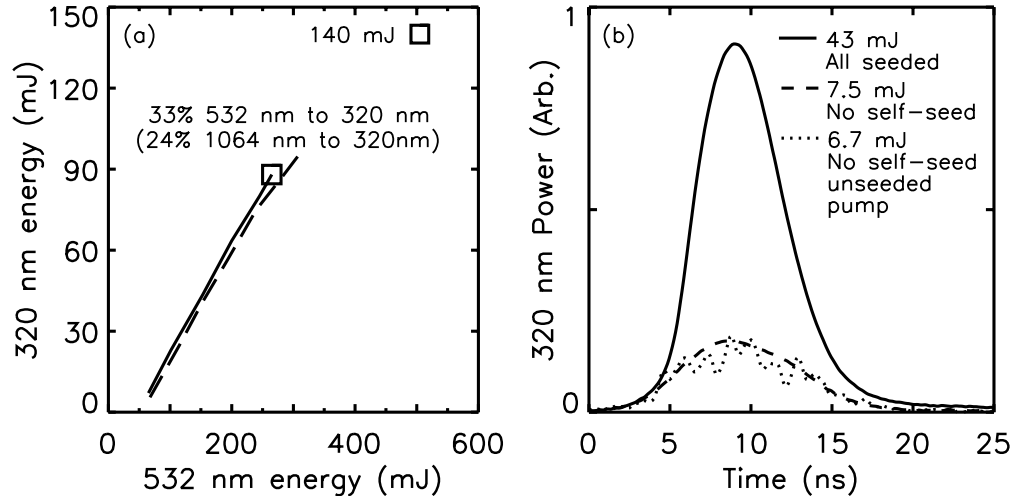
While the efficiency was higher than we achieved for extra-cavity SFG, the measured performance fell short of predictions by numerical models that indicated 532 nm to 320 nm conversion efficiency exceeding 50%.<sup>11</sup> However, this discrepancy was not unexpected in a “real world” device. Small deviations from optimum operating parameters such as the crystal lengths described in Sec. 3.1 can strongly affect competition between oscillation and SFG. Optimum SFG efficiency will be realized only when a delicate balance is maintained between these two competing processes.

Figure 3(a) shows measured efficiency curves for 320 nm energy versus the 532 nm pump energy, with two boxes indicating the highest measured efficiency and highest measured energy. UV energy was maximized by adjusting the OPO and SFG crystals to  $\Delta k = 0$ , and by interferometric alignment of the pulsed seed beam for maximum pump depletion. Externally triggered arrival times of the two pump pulses were adjusted to maximize pump depletion as well, with timing controlled to within 1–2 ns. The backward-propagating pump beam was aligned to overlap the cavity mode determined by the cw seed beam, and the forward-propagating pump beam aligned to the path of the backward pump. Two efficiency curves were recorded to check for reproducibility. From these data we determined maximum 532 nm to 320 nm efficiency of 33%, and given our Nd:YAG SHG efficiency of 70%, a 1064 nm to 320 nm efficiency of 24%. Although we’re pleased with these results, we believe they can be improved with small refinements. These include further optimization of pump beam quality, and perhaps replacing self-seeding at the signal wavelength with pulsed idler seeding. While self seeding is an effective method for increasing efficiency, an artifact in the form of an unwanted back-reflection at  $\lambda_{\text{signal}}$  that arises from backward pumping diminishes beam quality, which might effect OPO and SFG efficiency.<sup>4</sup> Pulsed idler seeding should eliminate the effects of this artifact, and it appears to be practical because numerical modelling suggests it requires pulse energies  $\leq 200$   $\mu$ J.

The pulse time profiles in Fig. 3(b) illustrate how self seeding enhanced the UV generation efficiency when the OPO was pumped just above its threshold for unseeded oscillation. The pulse shown by the solid line corresponds to a UV energy of 43 mJ, and was recorded with self seeding. The dashed line represents UV generation without self seeding and contains a comparatively small 7.5 mJ. The dotted line represents UV generation using a broadband pump without self seeding, and contains only 6.7 mJ.

#### 5. CONCLUSIONS

We built and tested a high efficiency source of 320 nm light based on intra-cavity SFG in a self-injection seeded image-rotating nanosecond RISTRA OPO. The four-mirror nonplanar ring cavity contained an  $xz$ -cut KTP crystal pumped by the 532 nm second harmonic of Nd:YAG to produce an 803 nm signal and 1576 nm idler, and a type-II BBO crystal that sum-frequency mixed the resonated 803 nm signal with 532 nm pump to generate 320 nm light. The OPO was pulse injection seeded using the technique of self seeding, where the OPO was initially pumped in the backward propagation direction to generate its own seed pulse. The good beam quality provided by image rotation, and the high efficiency obtained from self seeding, resulted in 532 nm to 320 nm



**Figure 3.** (a) Efficiency curves for 320 nm versus 532 nm forward-pump energy. The lower box represents the highest measured efficiency, and the upper box a single, isolated measurement of highest recorded energy. Two efficiency curves that terminate near the lower box, solid and dashed, were recorded to check for reproducibility. (b) Pulse time profiles illustrating how self seeding enhanced the efficiency of intra-cavity SFG when the forward pump fluence is set just above the OPO's threshold for unseeded oscillation. The solid curve corresponds to the self-seeded UV energy, the dashed curve the UV energy without self seeding, and the dotted curve the UV energy without self seeding and with a broadband pump pulse. See text for additional details.

conversion efficiency of 33%, and a maximum 320 nm pulse energy of 140 mJ. While these results indicate high-efficiency UV generation, our numerical model predicted 532 nm to 320 nm conversion efficiency exceeding 50%. We suspect the discrepancy between predicted and measured results is due to pump beam quality, and also due to an artifact in the form of an unwanted back-reflection from backward pumping that diminishes beam quality. The efficiency may be improved by optimizing pump beam quality and by replacing self seeding with pulsed idler seeding to eliminate the artifact. Pulsed idler seeding could also reduce complexity because the backward pump-laser and self seeding optical path could be replaced by an efficient, fiber-based communication-wavelength source at  $\lambda = 1576$  nm that delivers pulse energies  $\leq 200$   $\mu$ J.

## ACKNOWLEDGMENTS

Sandia is a multiprogram laboratory operated by Sandia Corporation, a Lockheed Martin Company for the United States Department of Energy's National Nuclear Security Administration under contract DE-AC04-94AL85000. Additional financial support for this work was provided by NASA Langley Research Center, Hampton, VA, USA.

## REFERENCES

1. A. V. Smith and D. J. Armstrong, "Nanosecond optical parametric oscillator with 90° image rotation: Design and performance," *J. Opt. Soc. Am. B* **19**, pp. 1801–1814, 2002.
2. A. V. Smith and M. S. Bowers, "Image-rotating cavity designs for improved beam quality in nanosecond optical parametric oscillators," *J. Opt. Soc. Am. B* **18**, pp. 706–713, 2001.
3. D. J. Armstrong and A. V. Smith, "Demonstration of improved beam quality in an image-rotating optical parametric oscillator," *Opt. Lett.* **27**, pp. 40–42, 2002.
4. D. J. Armstrong and A. V. Smith, "All solid-state high-efficiency source for satellite-based UV ozone DIAL," in *Lidar Remote Sensing for Environment Monitoring V*, U. Singh, K. Mizutani, eds. *Proc. SPIE* **5653**, 2004.
5. A. J. Campillo, "Internal upconversion and doubling of an optical parametric oscillator to extend the tuning range," *IEEE J. Quantum Electron.* **QE-8**, pp. 914–916, 1972.

6. G. T. Moore and K. Koch, "Optical parametric oscillations with intra-cavity sum-frequency generation," *IEEE J. Quantum Electron.* **29**, pp. 961–969, 1993.
7. E. C. Cheung, K. Koch, and G. T. Moore, "Frequency upconversion by phase-matched sum-frequency generation in an optical parametric oscillator" *Opt. Lett.* **19**, pp. 1967–1969, 1994.
8. A. Shirakawa, H. W. Mao, T. Kobayashi, "Highly efficient generation of blue-orange femtosecond pulses from intracavity-frequency-mixed optical parametric oscillator," *Opt. Comm* **123**, pp. 121–128, 1996.
9. G. T. Moore and K. Koch, "Optical parametric oscillation with detuned intra-cavity sum-frequency generation," *IEEE J. Quantum Electron.* **29**, pp. 2334–2341, 1993.
10. Y. Dikmelik, G. Akgün, and O. Aytür, "Plane-wave dynamics of optical parametric oscillation with simultaneous sum-frequency generation," *IEEE J. Quantum Electron.* **35**, pp. 897–912, 1999.
11. Numerical models for the RISTRA OPO are derived from the SNLO software package, which is written and distributed by Dr. Arlee V. Smith of Sandia National Labs. SNLO contains 17 different software tools that can be used for design and testing of OPA's, OPO's, and to calculate nonlinear crystal mixing parameters. SNLO can be downloaded free of charge from <http://www.sandia.gov/imrl/XWEB1128/xxtal.htm>. Special codes for various versions of the one- and two-crystal image-rotating RISTRA OPO, including those for intra-cavity SFG, SHG, and DFG, are available on request.
12. D. J. Armstrong and A. V. Smith, "Efficient all solid-state UV source for satellite-based lidar applications," in *Lidar Remote Sensing for Environment Monitoring IV*, U. Singh, ed. *Proc. SPIE* **5154**, pp. 31–45, 2003.
13. D. J. Armstrong and A. V. Smith, "150-mJ 1550-nm KTA OPO with good beam quality and high efficiency," in *Nonlinear Frequency Generation and Conversion: Materials, Devices, and Applications III*, K. L. Schepler and D. D. Lowenthal, eds. *Proc. SPIE* **5337**, pp. 71–80, 2004.
14. Y. He and B. J. Orr, "Narrowband tuning of a pulsed optical parametric oscillator by wavelength-selective feedback," presented at CLEO/QELS 2003, Baltimore, Maryland, USA, 2–6 June 2003.
15. M. Rahm, G. Ansett, J. Bartschike, T. Bauer, R. Beigang, and R. Wallenstein, "Widely tunable narrowlinewidth nanosecond optical parametric generator with self-injection seeding," *Appl. Phys. B* **79**, pp. 535–538, 2004.
16. D. J. Armstrong and A. V. Smith, "Using a Newport refractive beam shaper to generate high-quality flat-top spatial profiles from a flashlamp-pumped commercial Nd:YAG laser," in *Laser Beam Shaping V*, F. M. Dickey, D. L. Shealy, and J. M. Sasián eds. *Proc. SPIE* **5525**, pp. 88–97, 2004.